The micro-RWELL technology: status and perspectives

G. Bencivenni[a], G. Felici[a], R. Farinelli[b], M. Gatta[a], L. Lavezzi[c],
G. Morello[a], R. de Oliveira[d], M. Poli Lener[a], A. Ochi[e]

a. LNF-INFN
b. INFN-Fe
c. IHEP Beijing
d. CERN
e. Kobe University

56th International Winter Meeting on Nuclear Physics, Bormio
January 23rd, 2018

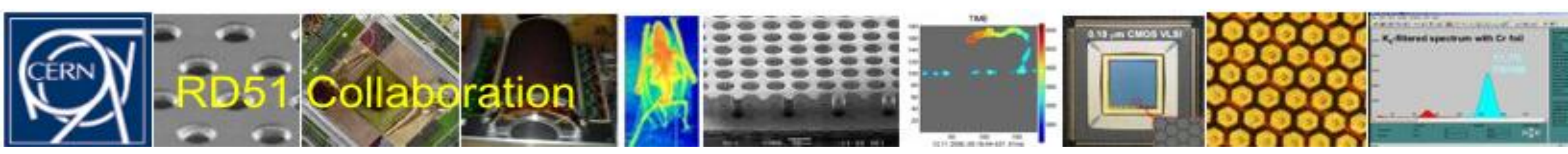

The µ-RWELL detectors

- They are composed of two elements: a **cathode** glued on a **frame**, working as spacer and as limit for the conversion gas volume, and the **µ-RWELL_PCB**
- The **µ-RWELL_PCB** is the core of the detector: this talk reports about its different versions developed taking into account the requirements of applications/experiments

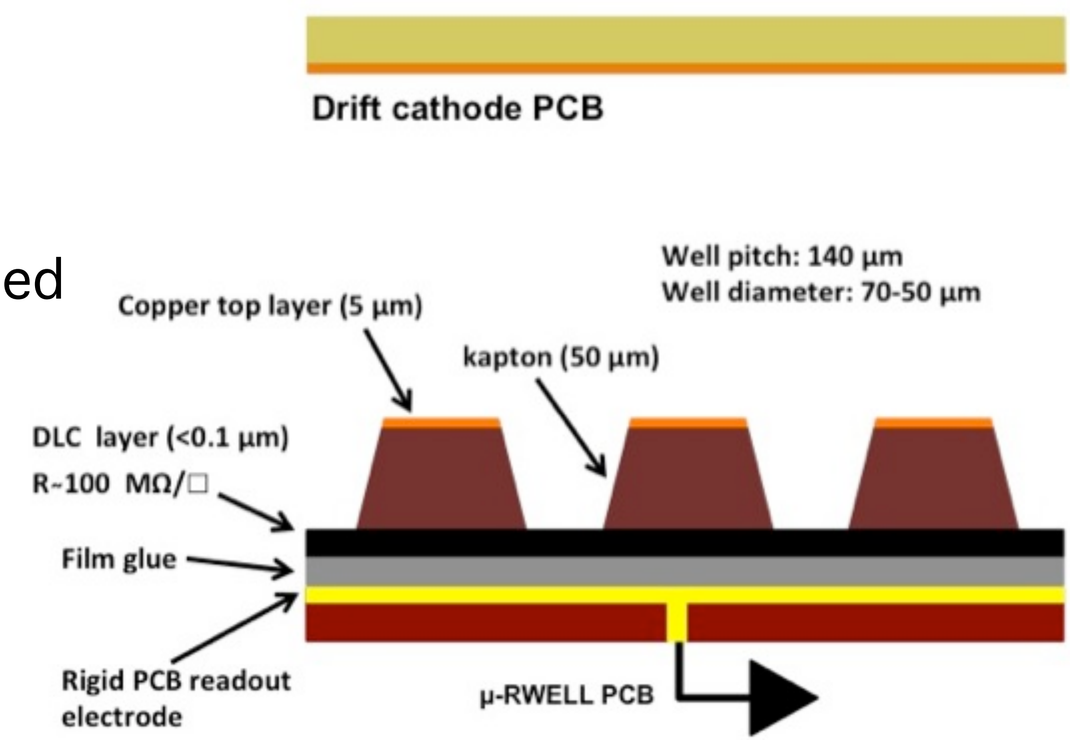

Why the resistive?

Because of the micrometric distance between electrodes, every MPGD suffers from spark occurrence that can damage the detector or the FEE.

A resistive readout quenches the discharge:

- The Raether limit is overcome
- The charge is deposited on the resistive layer
- The charge density spreads with $\tau = RC$

(M.Dixit, NIM A 518 (2004) 721)

- The resistive layer is locally charged-up with a potential $V=Ri$, reducing the ΔV applied to the amplification stage
- The amplification field is reduced
- The discharge is locally suppressed

Obviously this has a drawback correlated to high particle fluence, that's why we studied the performance of the detector as a function of the resistivity

The single resistive layer

- The simplest version of the detector, actually the first one, has been extensively studied with several prototypes each characterized by different surface resistivities [JINST 10 P02008, NIM A 824 (2016) 565]
- In this case the etched kapton foil, sputtered with DLC, is coupled through an insulating layer to the readout plane

5 μm Cu
50 μm Kapton
500 – 700 nm DLC
50 μm pre-preg

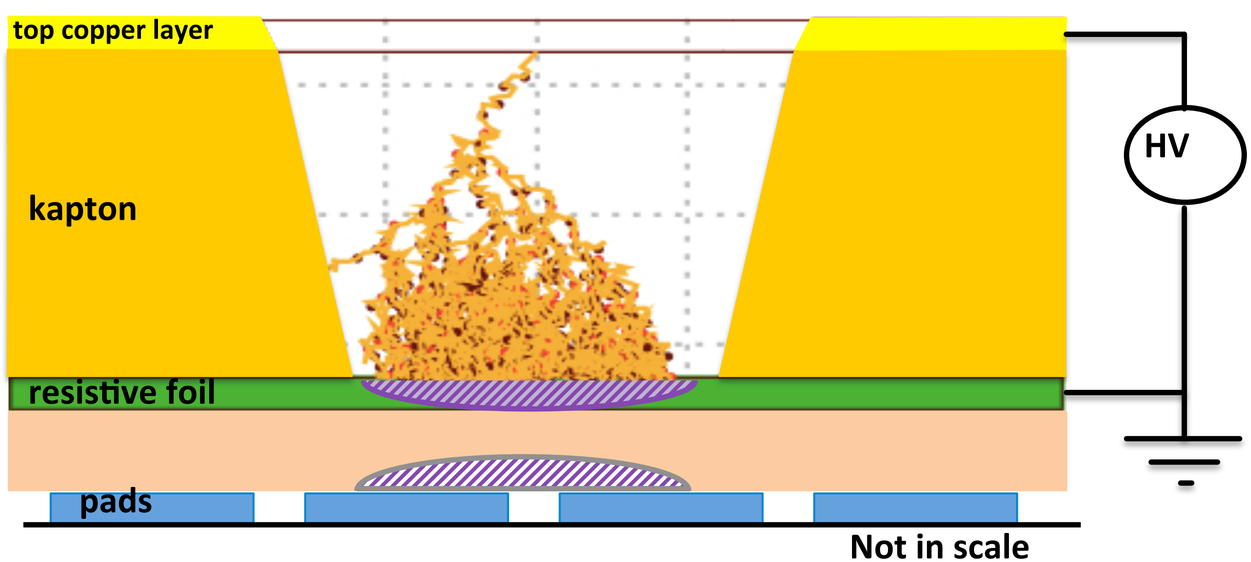

Status of the single resistive layer

Several measurements have been already reported [PoS(Bormio2017)002]: gas gain, space resolution for orthogonal particle, time resolution and gain drop.

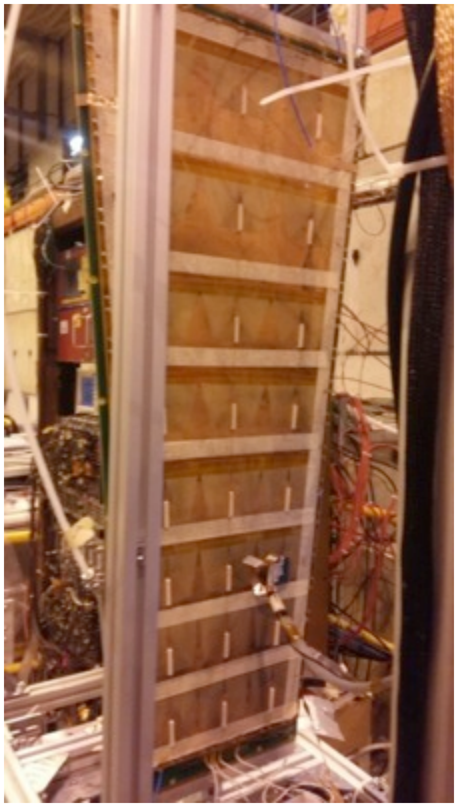

The R&D on the single resistive layer has been completed with the realization of two large area detectors of about **1.2 x 0.5 m^2** in the framework of the CMS-phase2 muon upgrade

These detectors have been realized in collaboration with Italian companies (ELTOS & MDT) within the TT project

Missing: space resolution with non-orthogonal tracks and R&D on the high rate scheme

Improving space resolution: the µ-TCP mode

The use of an analogic front-end allows to associate a hit to a track using the charge centroid (CC) method. The uncertainty associated to the hit with this algorithm is dependent on the track angle: minimum for orthogonal tracks and larger as the angle increases

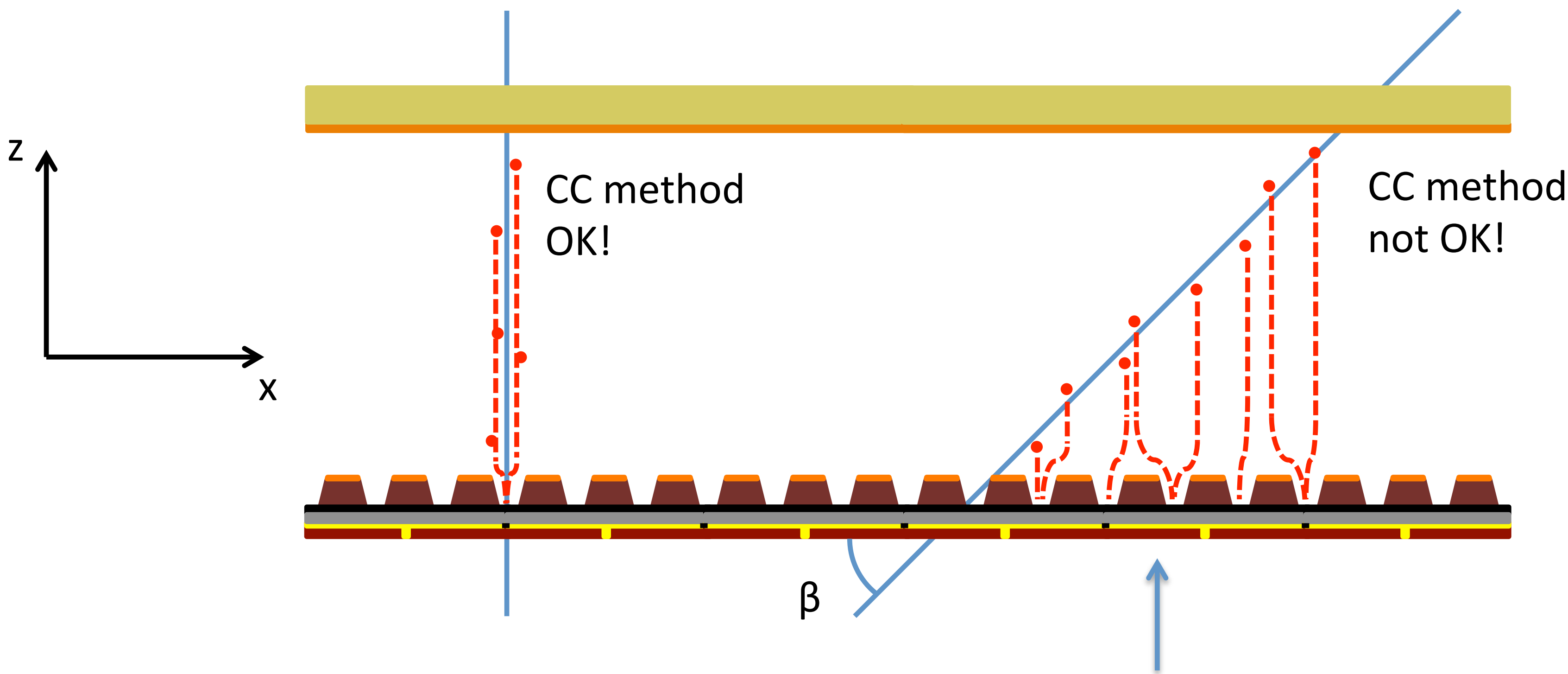

To improve the space resolution we implemented the u-TPC algorithm to be combined with the CC method

Improving space resolution: the μ-TCP mode

Introduced for MicroMegas by T. Alexopoulos et al., NIM **A 617** (2010) 161, it suggests a way to overcome big errors associated to sloped tracks.

Each hit is projected inside the conversion gap, where the x position is given by each strip and the $z = v_d t$

The drift velocity is provided by the Magboltz libraries.

The drift time is obtained with a fit of the charge sampled every 25 ns (APV25) from each FEE channel associated to the strip.

For each event we then obtain a set of projected hits that once fitted provide a track segment

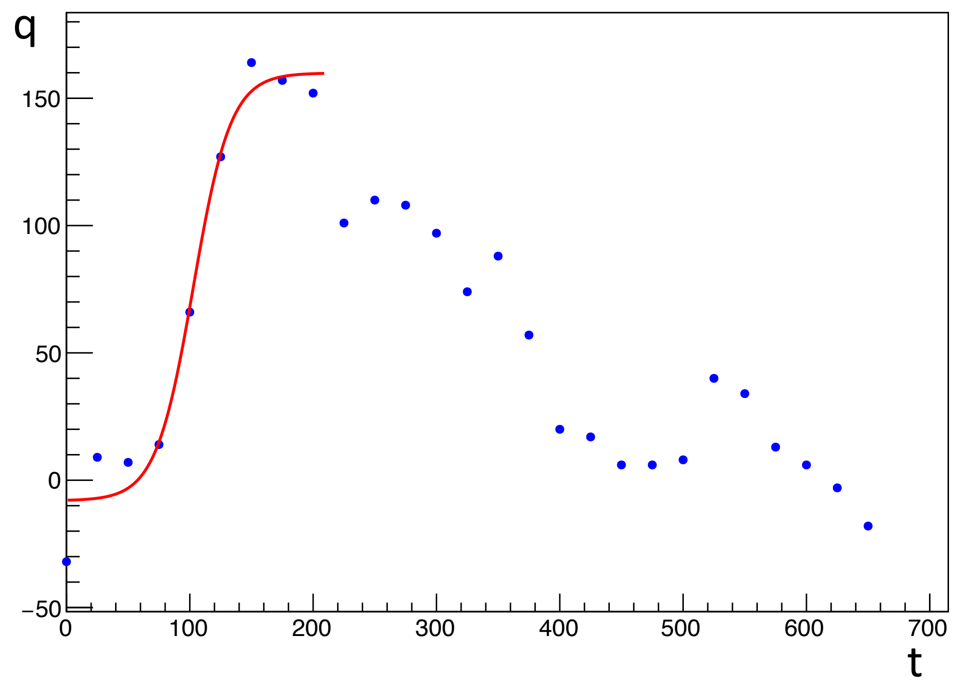

Example of μ-TPC reconstruction

Here we have some examples where the tracks have an angle w.r.t. the readout plane of:

75° tracks

45° tracks

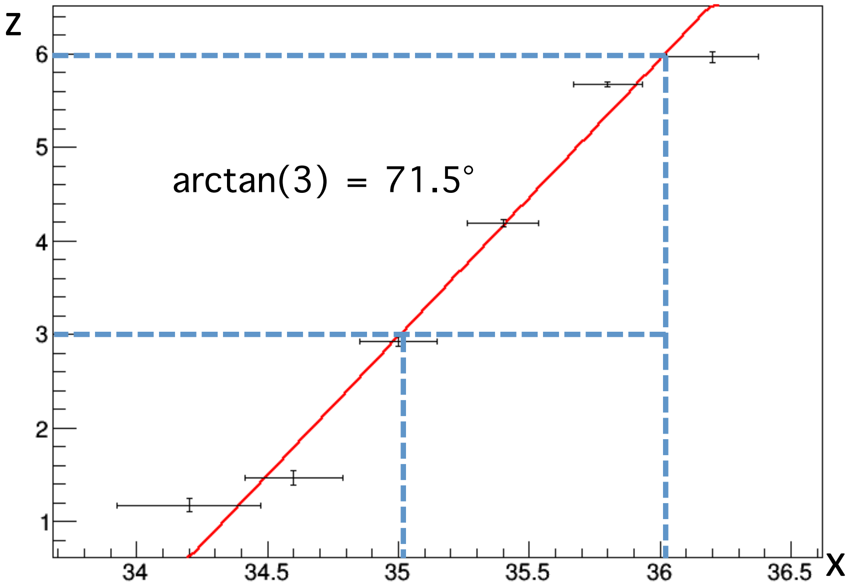

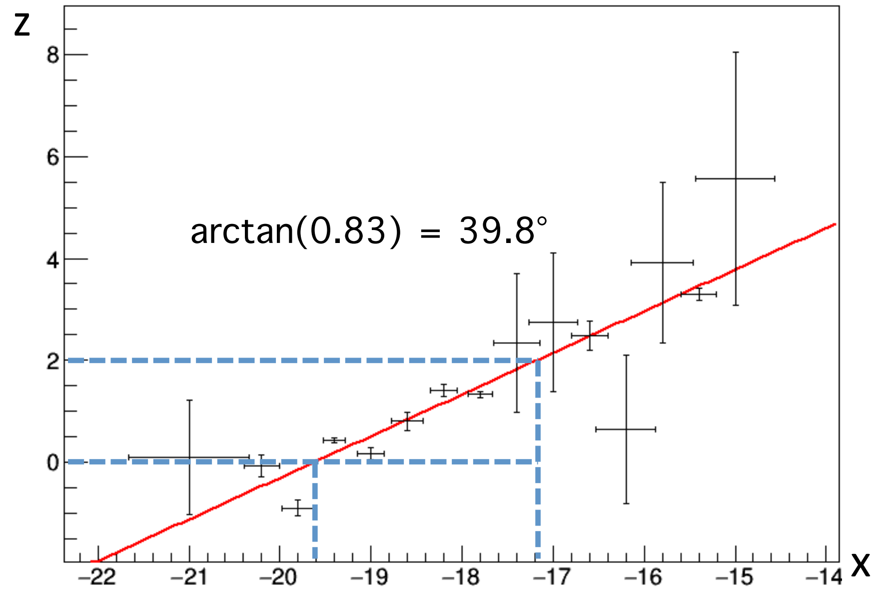

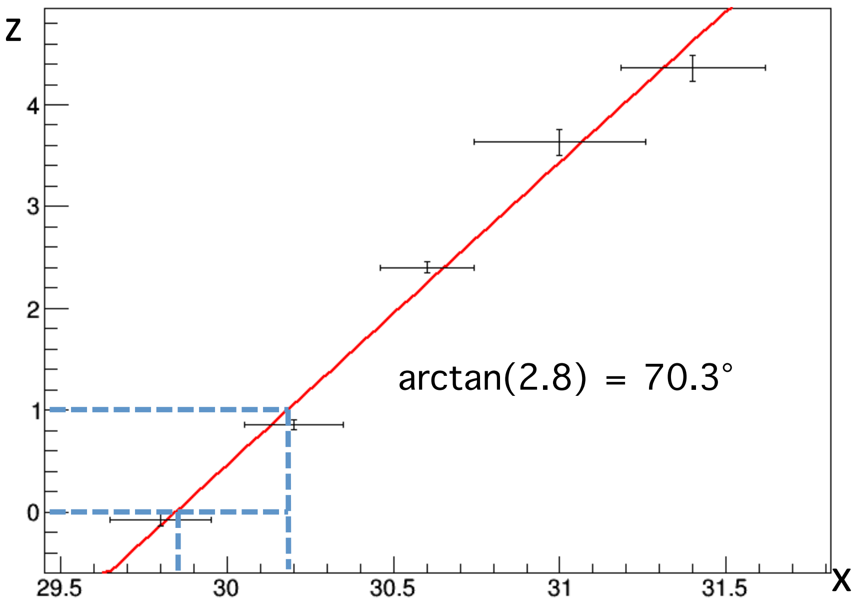

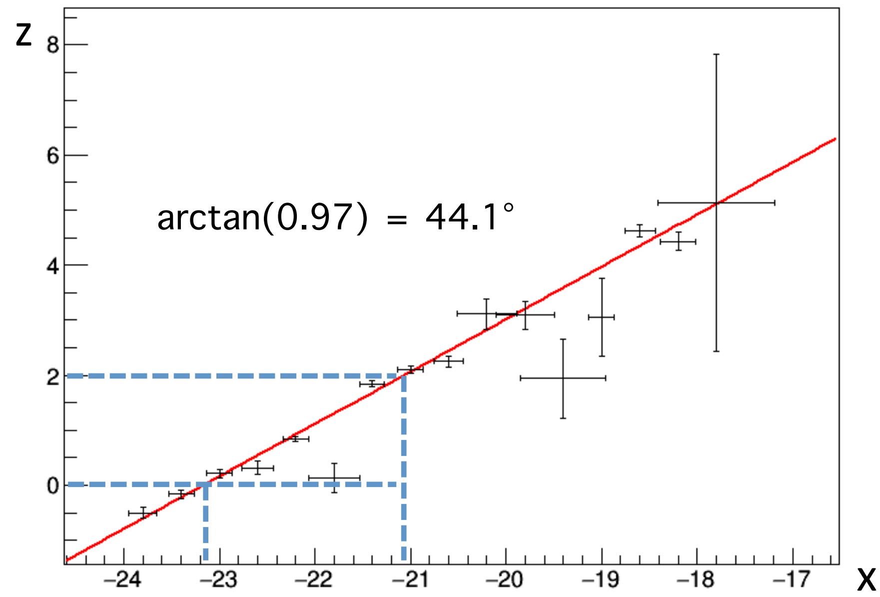

Improving space resolution: the μ-TCP mode

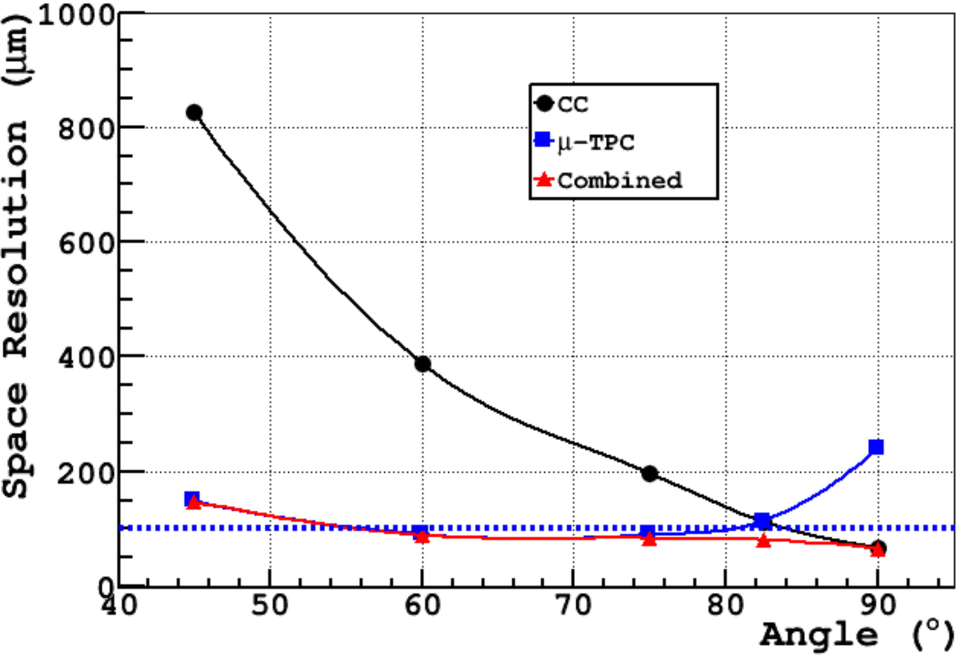

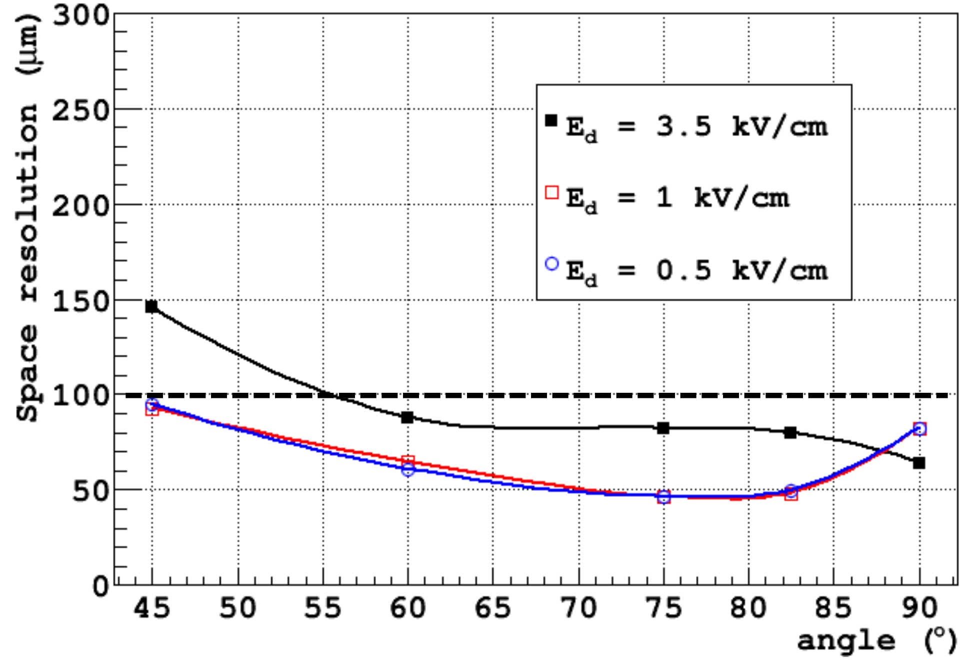

The combination of the CC and the μ-TPC mode with E_d= 3.5 kV/cm
The resolution is flattened for a wide range of angles.

$$x_{merge} = \frac{x_{cc} \cdot w_{cc} + x_{tpc} \cdot w_{tpc}}{w_{cc} + w_{tpc}}$$

$$w_{cc} \propto (clsize)^{-2} \quad w_{\mu-TPC} \propto (clsize)^2$$

A study on the optimization of the drift field: low fields correspond to low drift velocities, allowing a better resolution of the primary ionization clusters.

High rate version: the double resistive layer

- The charges collected on the resistive layer move towards the ground with a characteristic time τ(R,C) [Dixit et al, NIMA 518 (2004) 721, NIMA 566 (2006) 281].
- The idea is to reduce the path covered by the electrons on the DLC

5 μm Cu
50 μm Kapton
500 – 700 nm DLC
10 μm epoxy
500 – 700 nm DLC
50 μm epoxy

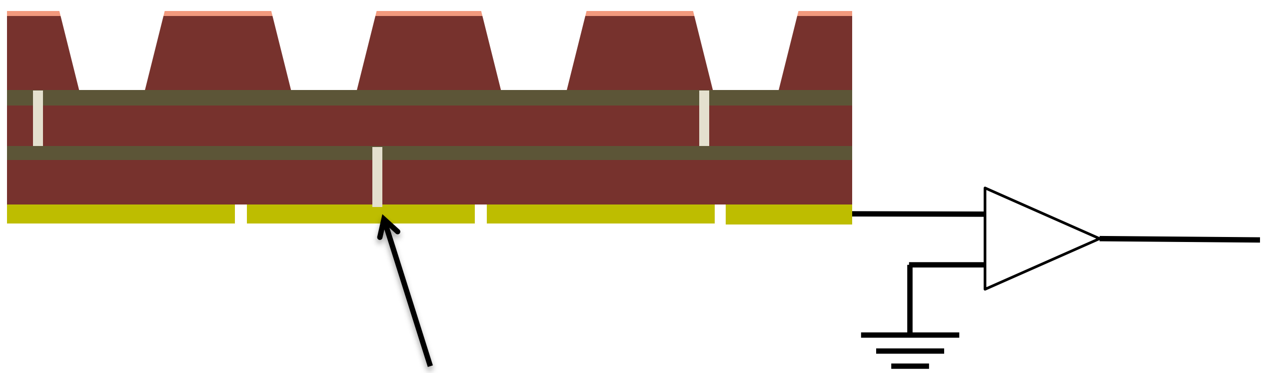

A matrix of conductive vias connects the two resistive layers. Another matrix of vias chains the second resistive layer to ground through the readout

The double resistive layer:

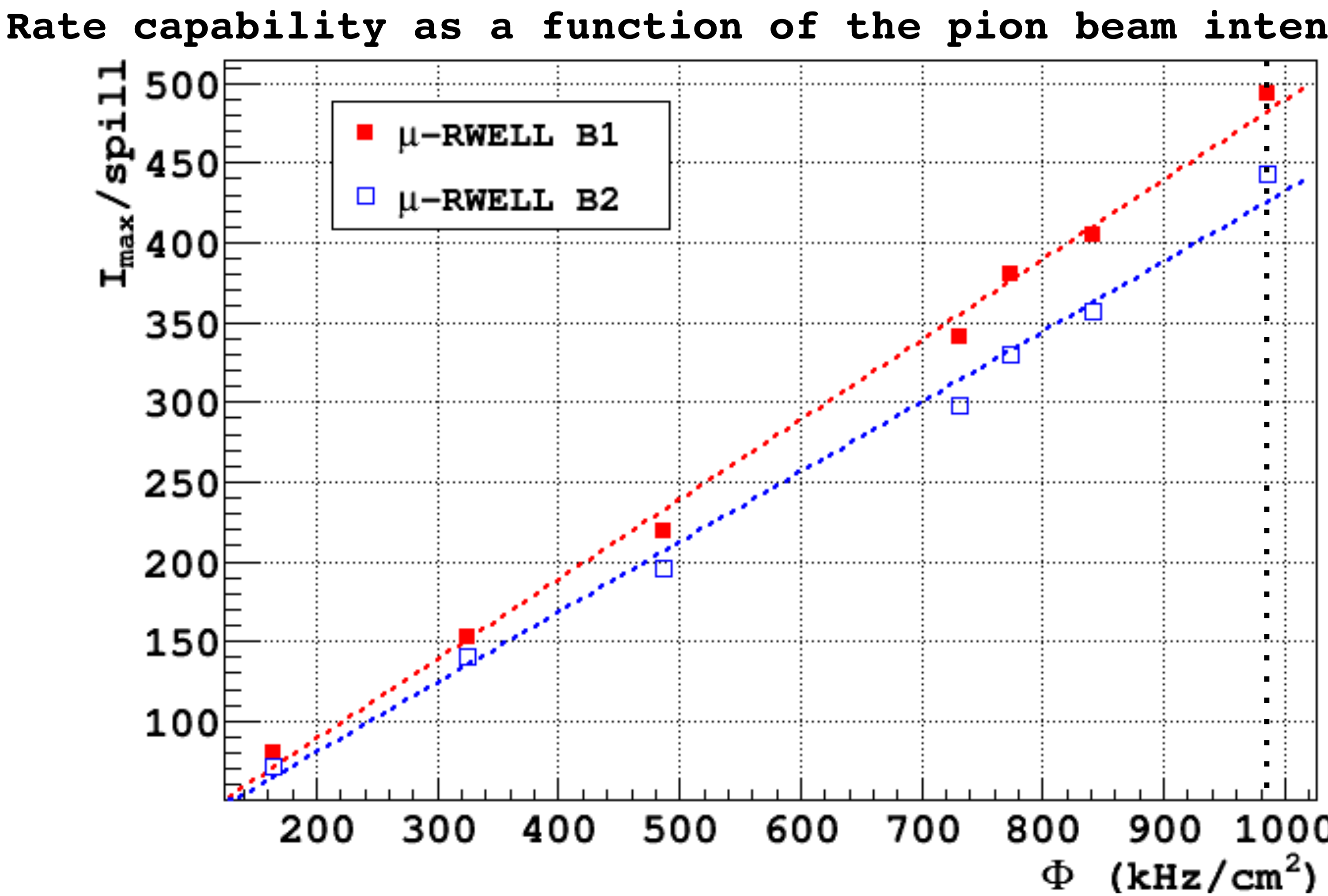

Detectors operated at a gain of 10^4. Beam spot ~2 cm^2 (RMS^2)

Status of the technological transfer

- As already mentioned, the strict collaboration with **ELTOS** made possible the construction of large area detectors with single resistive layer (GE1/1-, GE2/1-like)

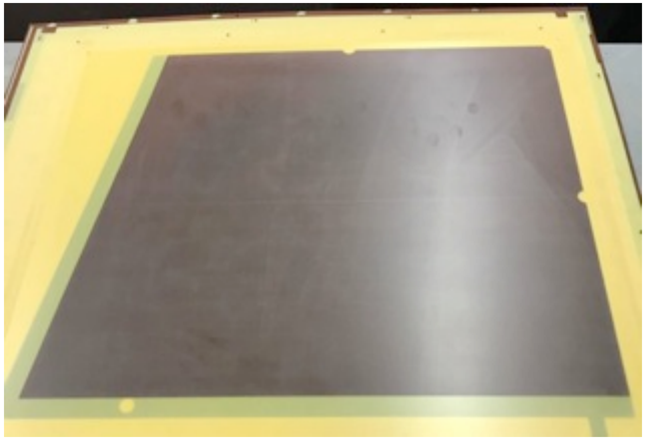


- This allowed us to well define the coupling procedure of the amplification stage with the readout
- ELTOS is now producing other μ-RWELL_PCB to be etched at CERN
- The industrialization of the double resistive layer construction is much more difficult due to the manufacturing of the conductive vias
- Other (simpler) layouts must be developed in order to be included in an industrial process

New layouts, new ideas, new challenges

The aim is to maintain a very short path for charges drifting on the resistive layer, while simplifying the construction process.

Two ideas are now under development: silver grid and resistive grid

Silver Grid (SG)

Small conductive strips are screen-printed on the bottom part of the DLC

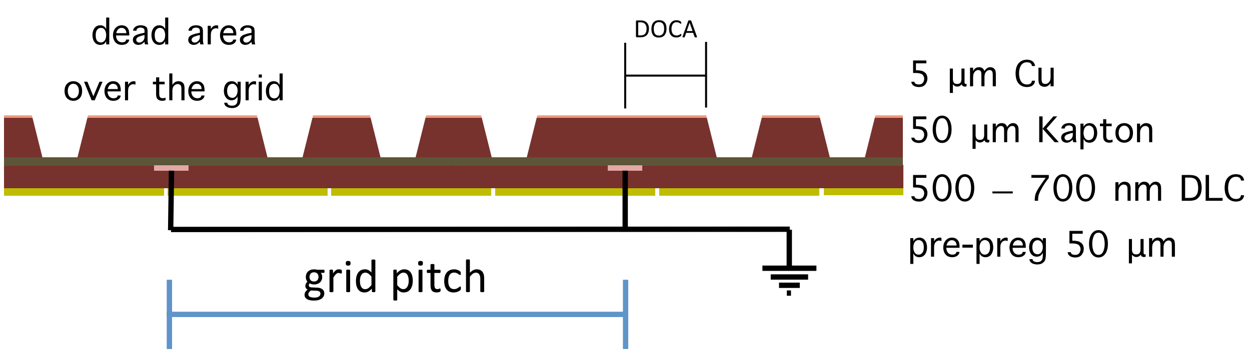

Clearly the introduction of a conductive strip on the bottom layer of the amplification stage can induce strong instabilities due to discharges over the DLC surface.

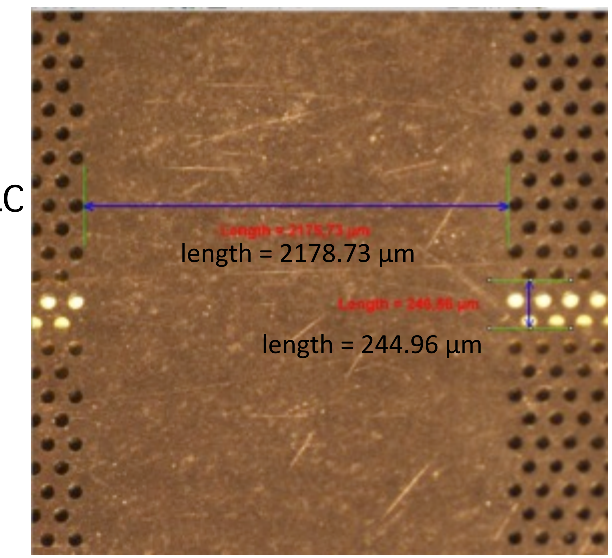

First prototypes of SG designed with safe geometrical parameters: grid pitch 6 mm, dead area around 1/3 of the total area

Silver Grid v1:
X-rays and H4 test beam (July 2017)

- A SG μ-RWELL has been installed inside the RD51 tracking system and characterized together with a Double Layer chamber

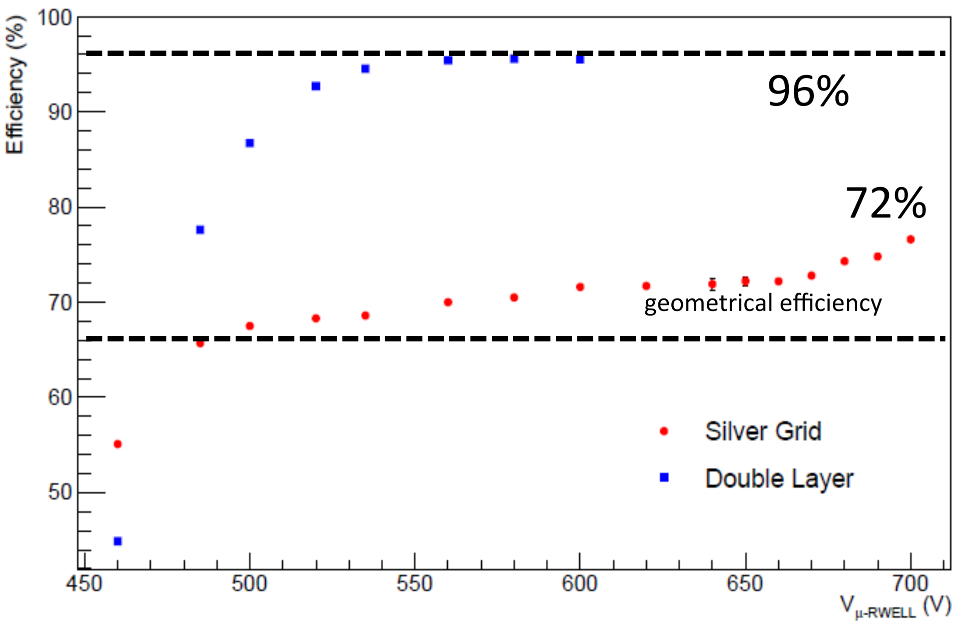

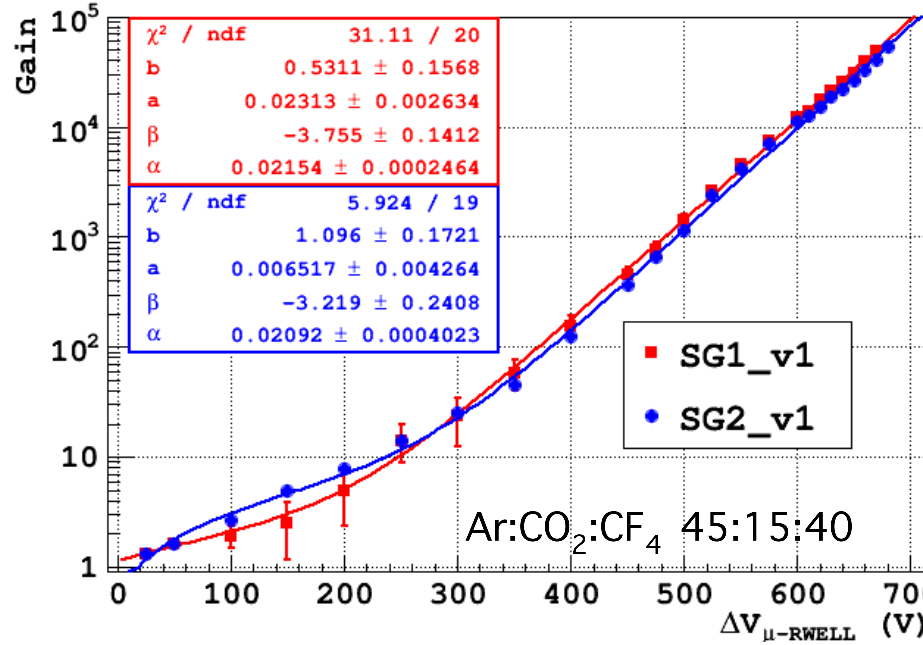

At the H4 test beam we could supply **up to 700 V**, much more than for the other μ-RWELL without instabilities. The reason of a so high instability voltage is **under investigation**.

The lower efficiency is due to the geometrical effects. The increasing gain improves the collection efficiency partially compensating this leak.

A dedicated study on the minimum distance between the strip and the holes has been done to increase the efficiency

Silver Grid: optimization

In order to reduce the dead area, we measured the Distance Of Closest Approach (without discharges) between two tips connected to a PS. We recorded the minimum distance as a function of the ΔV supplied for different foils before a discharge on the DLC occurs

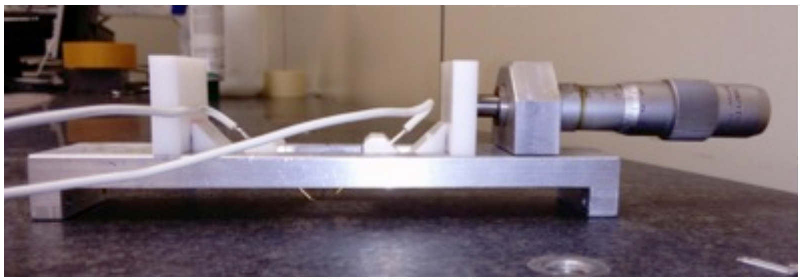

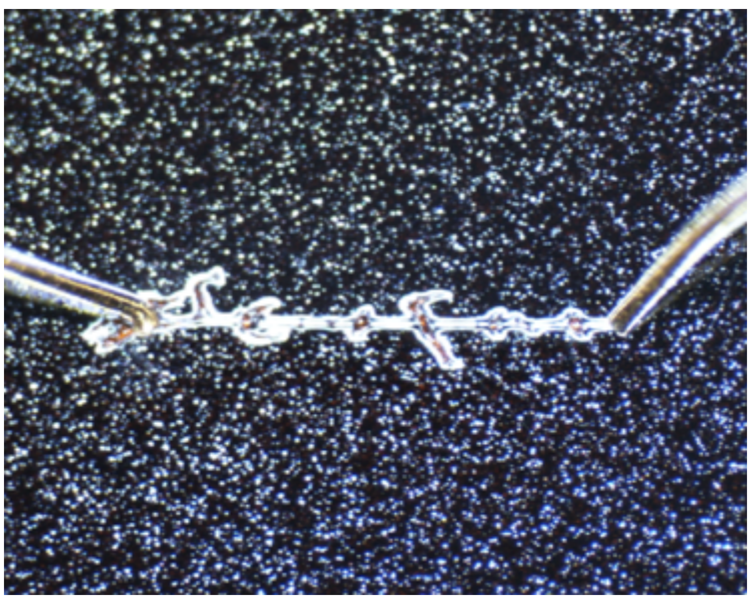

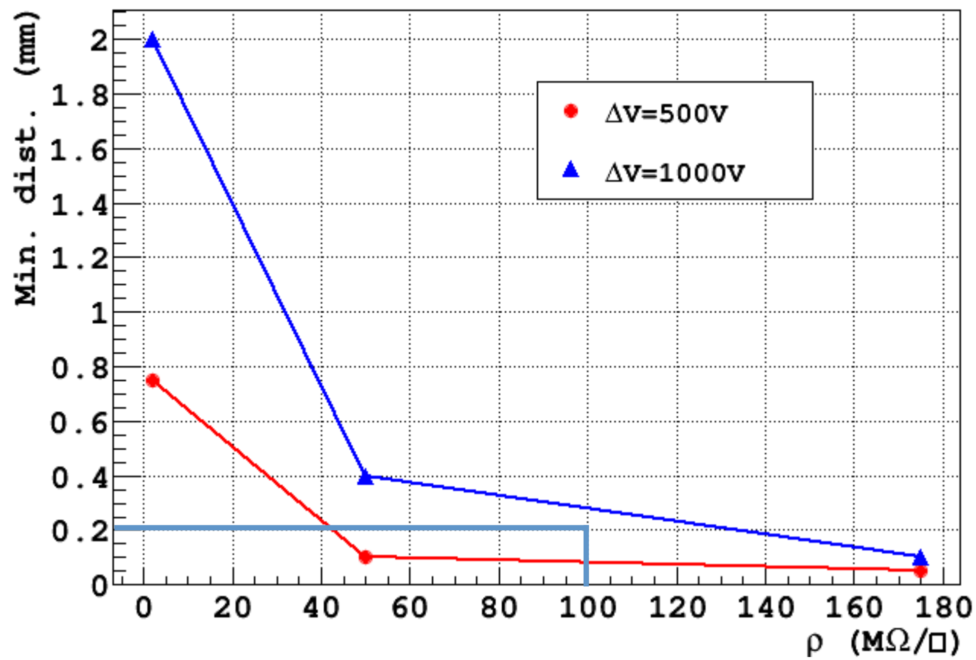

Two more prototypes delivered in November, with grid pitch 12 mm, dead area 1/10 of the active area

Silver Grid: 2^{nd} generation

The two detectors have been equipped with 6 x 8 mm^2 pad-segmented readout

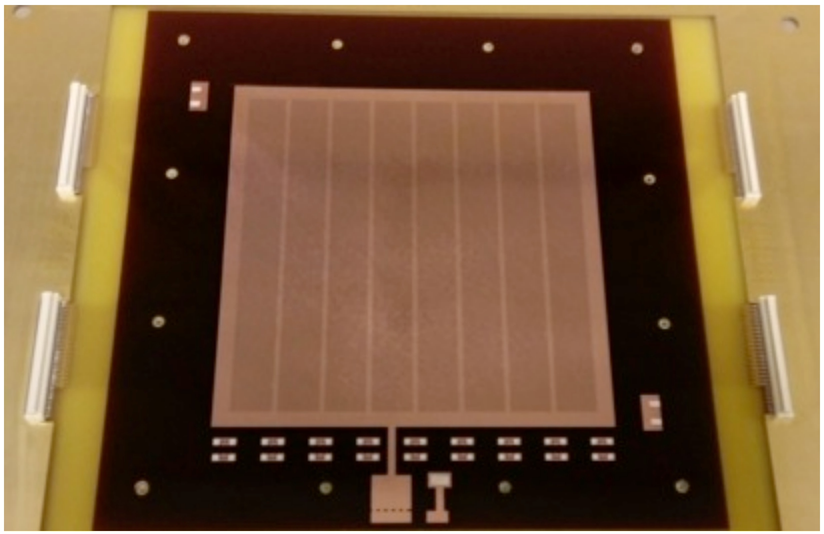

The grid lines are connected to the ground through the resistance provided by the DLC itself (9-10 MΩ)

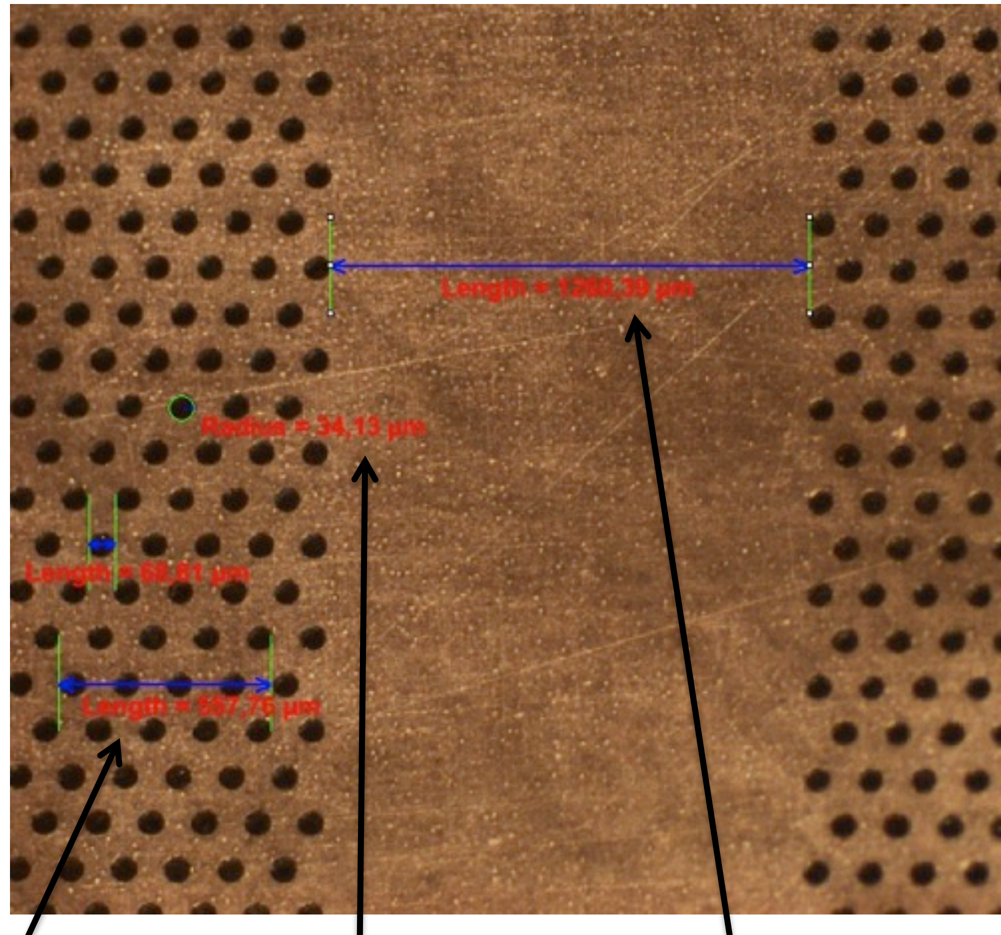

Silver Grid: 2nd generation

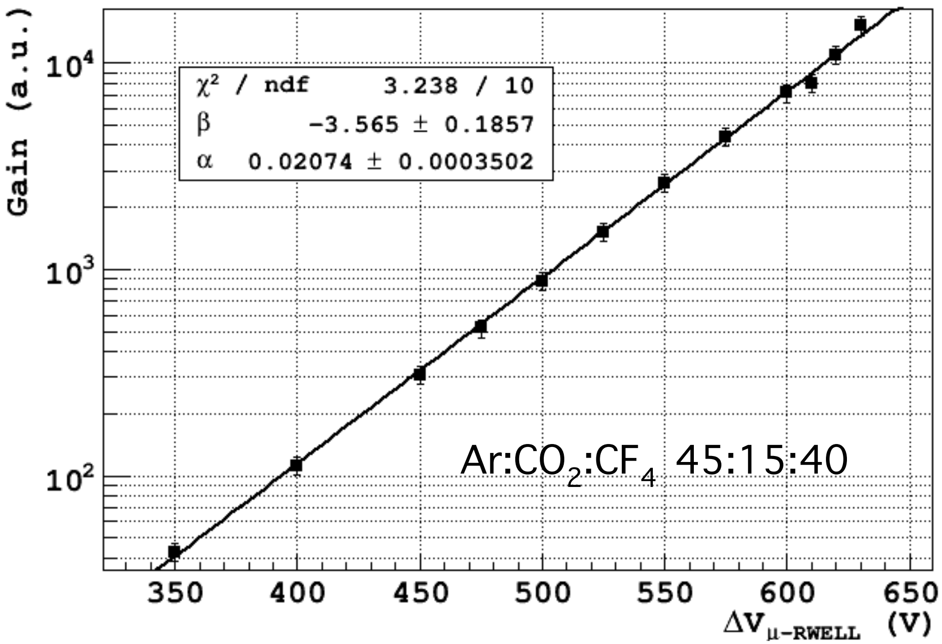

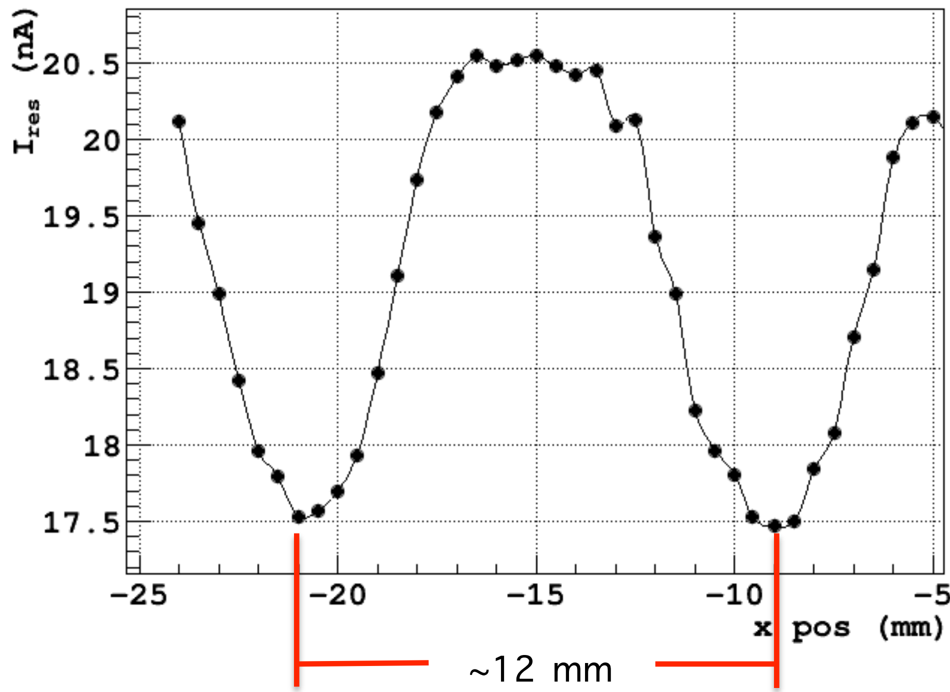

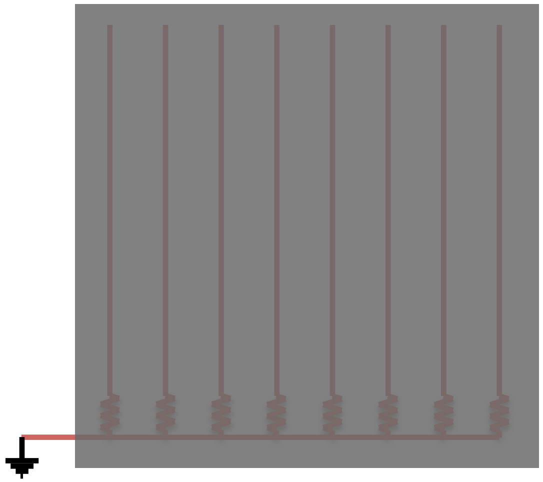

The detector is mounted on a support moved by a stepper motor. The position is given within few tenths of millimeter.

Scan along the coordinate orthogonal to the grid lines direction

Resistive grid

Small resistive strips are screen-printed on the bottom side of DLC

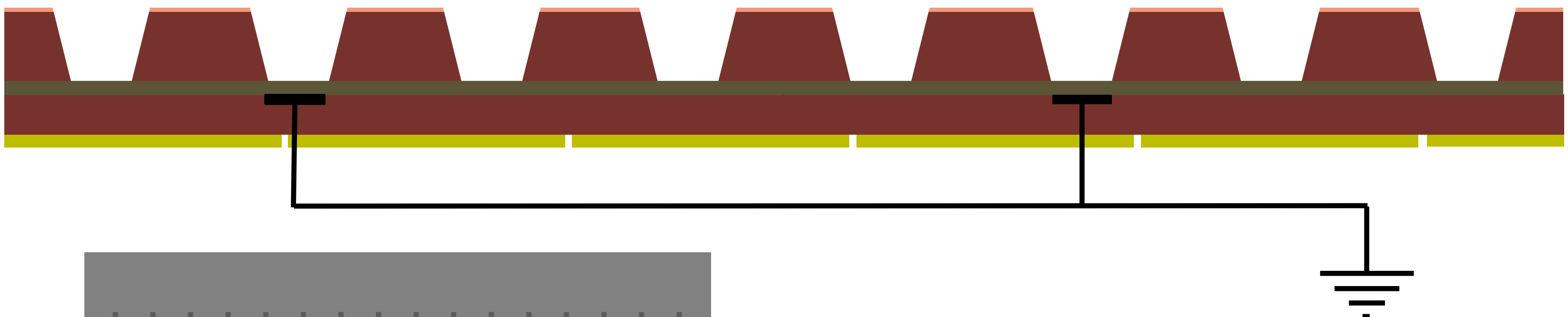

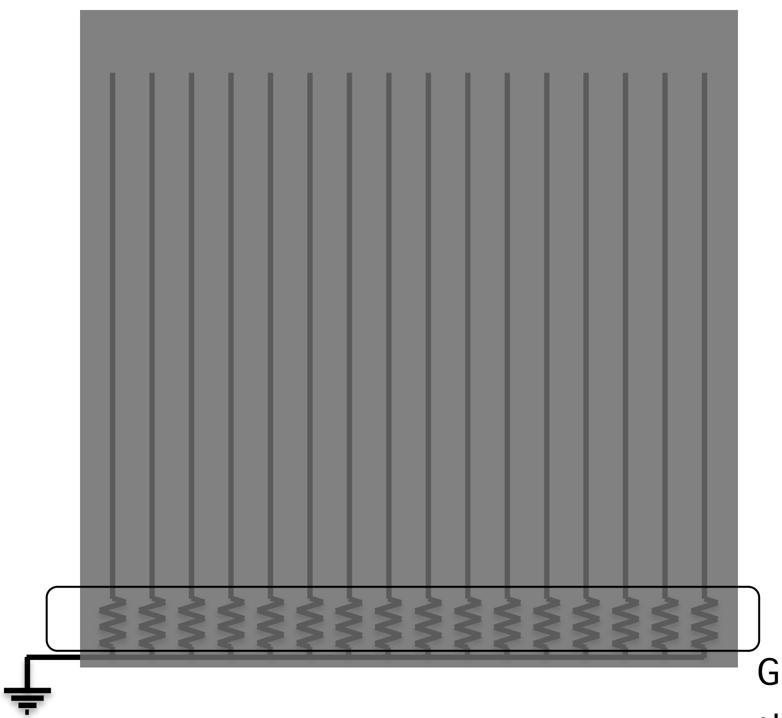

The grid grounding is similar to the one used for the 2nd generation SG, as well as the readout segmented in pads.

Two prototypes designed with 6 mm grid pitch

Resistive grid

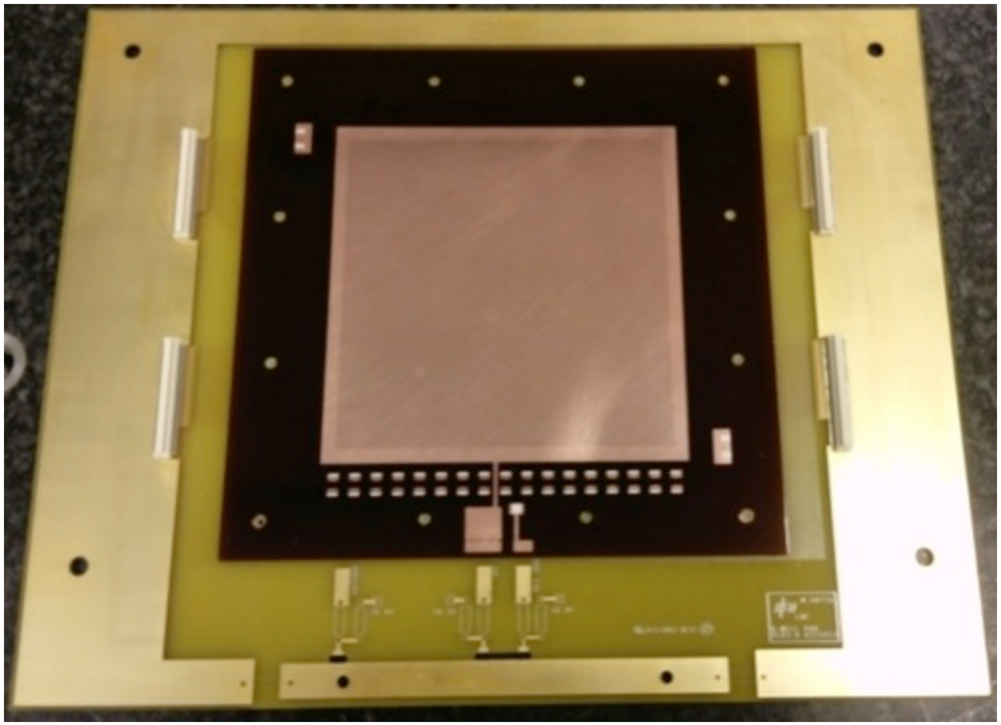

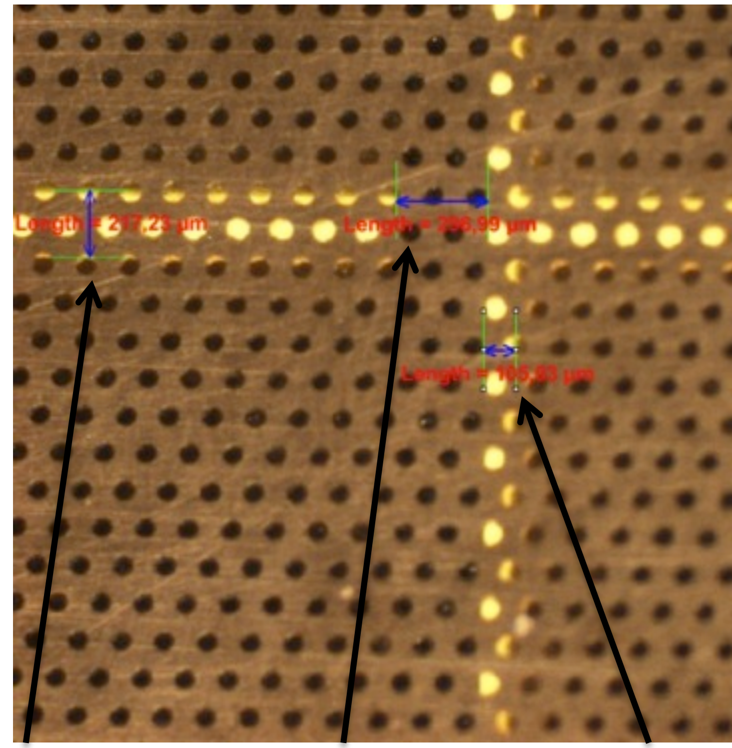

No dead areas

Y distance of pads: 217.23 µm

Resistive strip width: 296.99 µm

X distance of pads: 105.03 µm

Grounding resistance: between 12 and 16 MΩ

Gain drop measurement with 5.9 keV X-ray

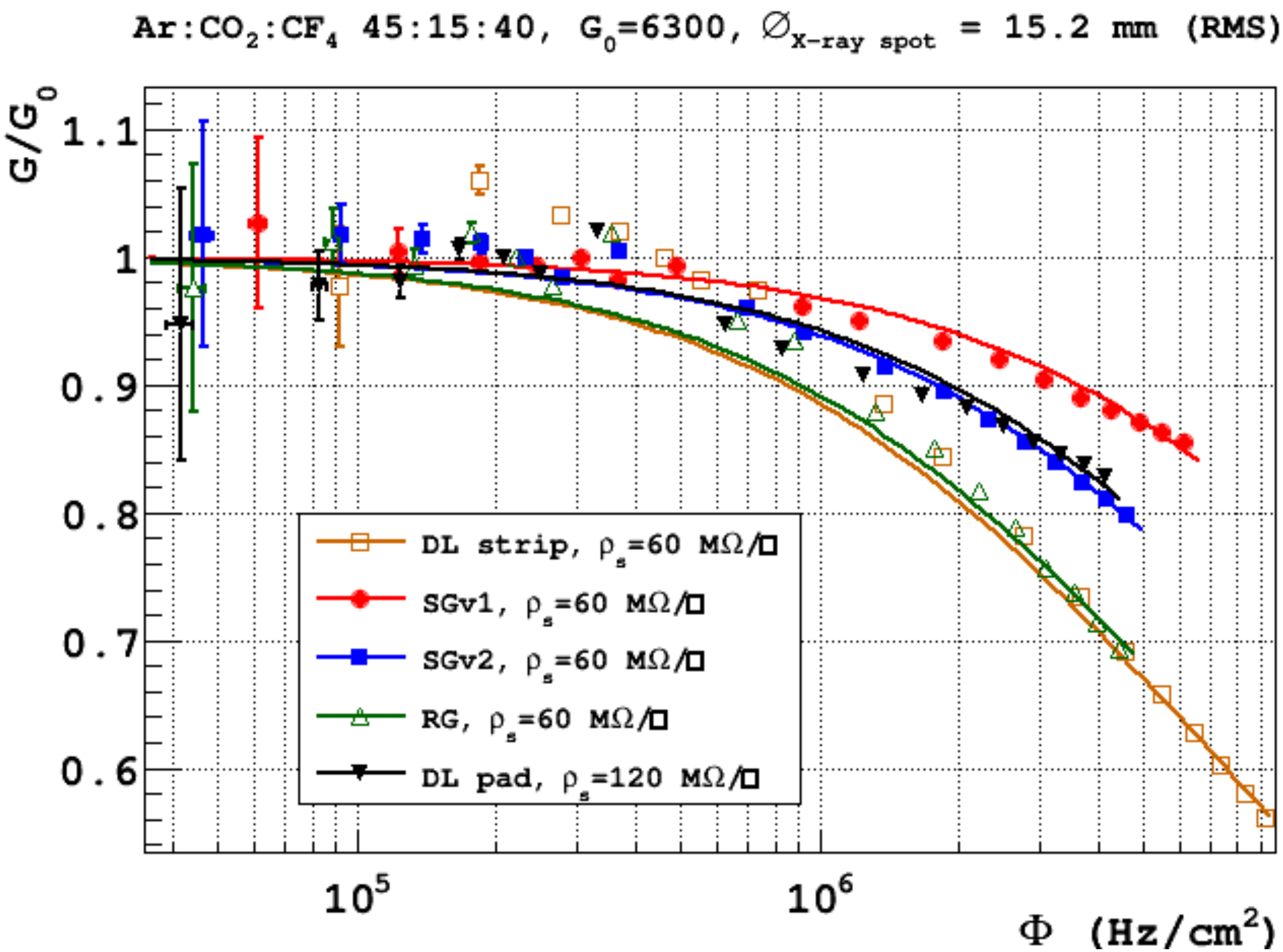

The gain drop is only due to Ohmic effect on the resistive layer: the charges collected on the DLC drift towards the ground facing an effective resistance Ω, depending on the evacuation scheme and computed by the parameter p_0

$$\frac{G}{G_0} = \frac{-1+\sqrt{1+4p_0\Phi}}{2p_0\Phi}$$

Gain drop and efficiency

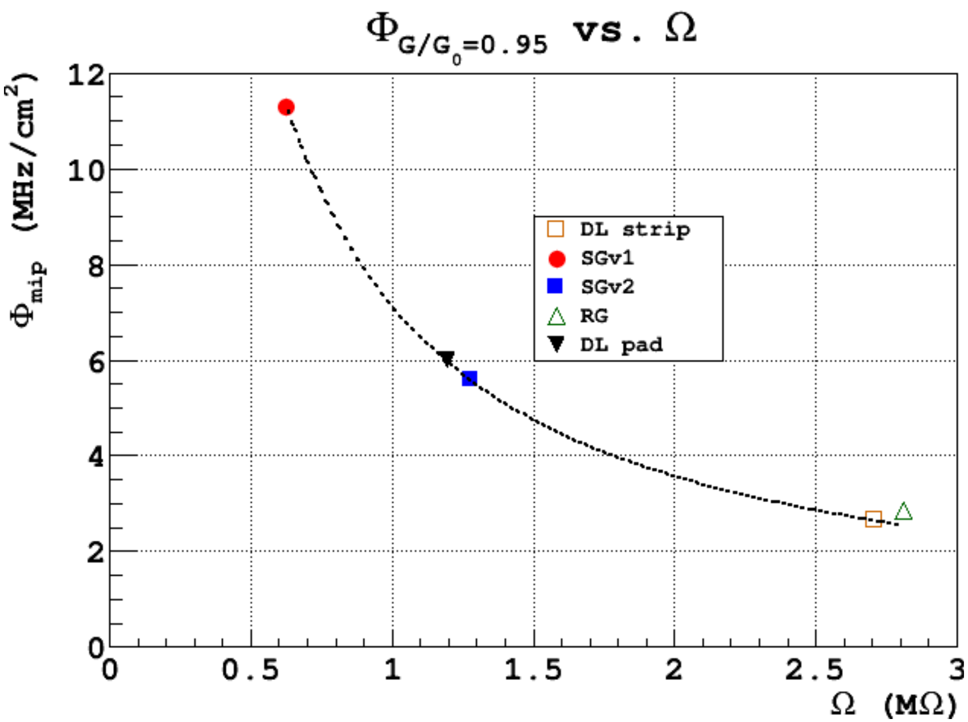

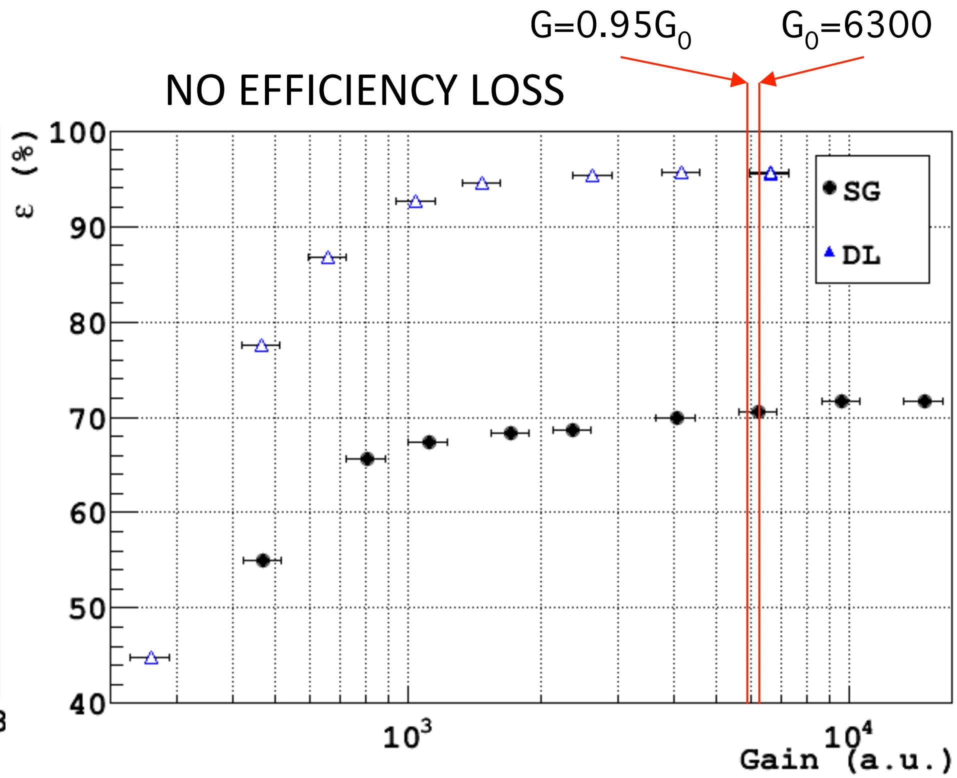

The primary ionization of 5.9 keV is ~7 times larger than the one created by a m.i.p. In order to face a **3 MHz/cm^2 m.i.p. fluence, with a 5% gain drop,** the effective resistance Ω must be at maximum 2 MΩ.

Anyway a 5% drop of G_0=6300 allows still to operate the detector at full efficiency. A measurement of the efficiency with a high rate particles has been planned for the next test beam

Conclusions & outlook

- The single layer layout has been exploited to build large area detectors (~1/2 m^2), but we also demonstrated that even larger detectors can be realized with the splicing technique, with the cooperation with ELTOS SpA, within TT
- Several prototypes have been realized, with different simplified evacuation charge scheme for high rate purposes
- Further optimization of the new high rate schemes must be done, addressed by the measurement of the gain drop done with X-rays

So far the best measured performances are:

- 1 MHz/cm^2 rate capability with pion beam (Double Layer working at G=10000)
- space resolution 52 ± 6 μm (80 MΩ/□, orthogonal tracks, no B field)
- well below 100 μm with non-orthogonal tracks, with the μ-TPC/CC combination
- time resolution 5.7 ns (with FEE saturation)
- Both the Silver Grid v1 reached a gain of almost 10^5 (to be understood)
- **An ageing test at GIF++** is ongoing: the detector integrated up to 90 mC/cm^2 without showing gain loss

Spare

The two different schemes

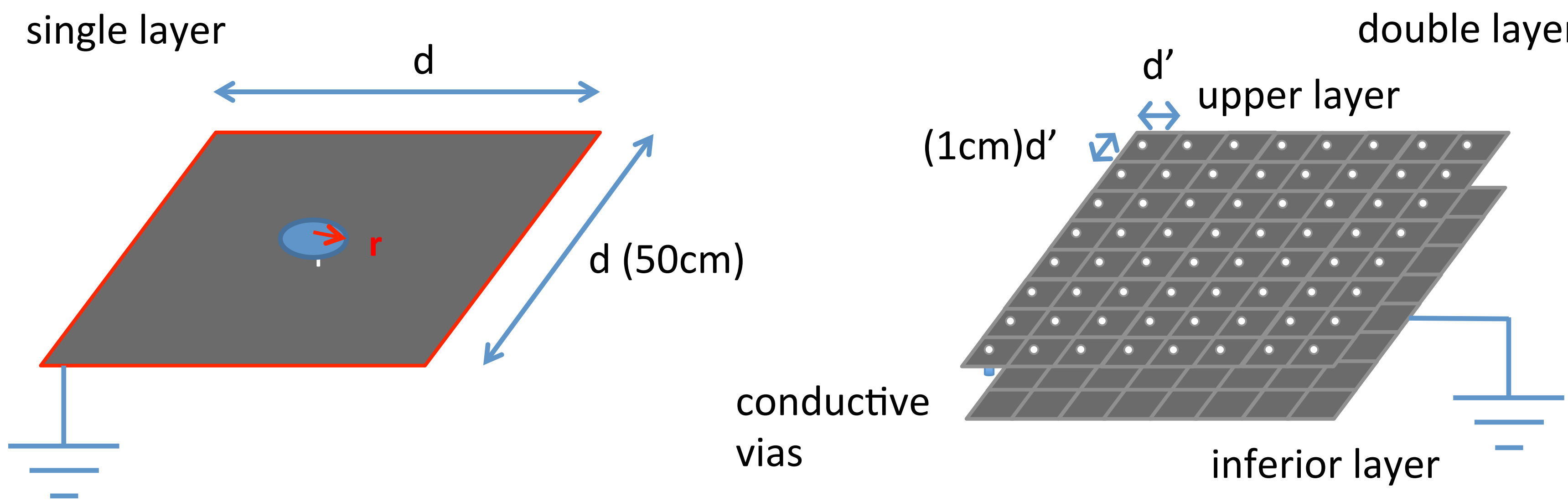

(*) point-like irradiation, r<<d
Ω is the resistance seen by the current generated by a radiation incident in the center of the detector cell

$$\Omega \sim \rho_s \times d/2\pi r \qquad \Omega' \sim \rho_s' \times 3d'/2\pi r$$

$$\Omega/\Omega' \sim (\rho_s/\rho_s') \times d/3d'$$

$$\text{If } \rho_s = \rho_s' \rightarrow \Omega/\Omega' \sim \rho_s/\rho'_s * d/3d' = 50/3 = 16.7$$

appendix A-B (G. Bencivenni et al., 2015_JINST_10_P02008)

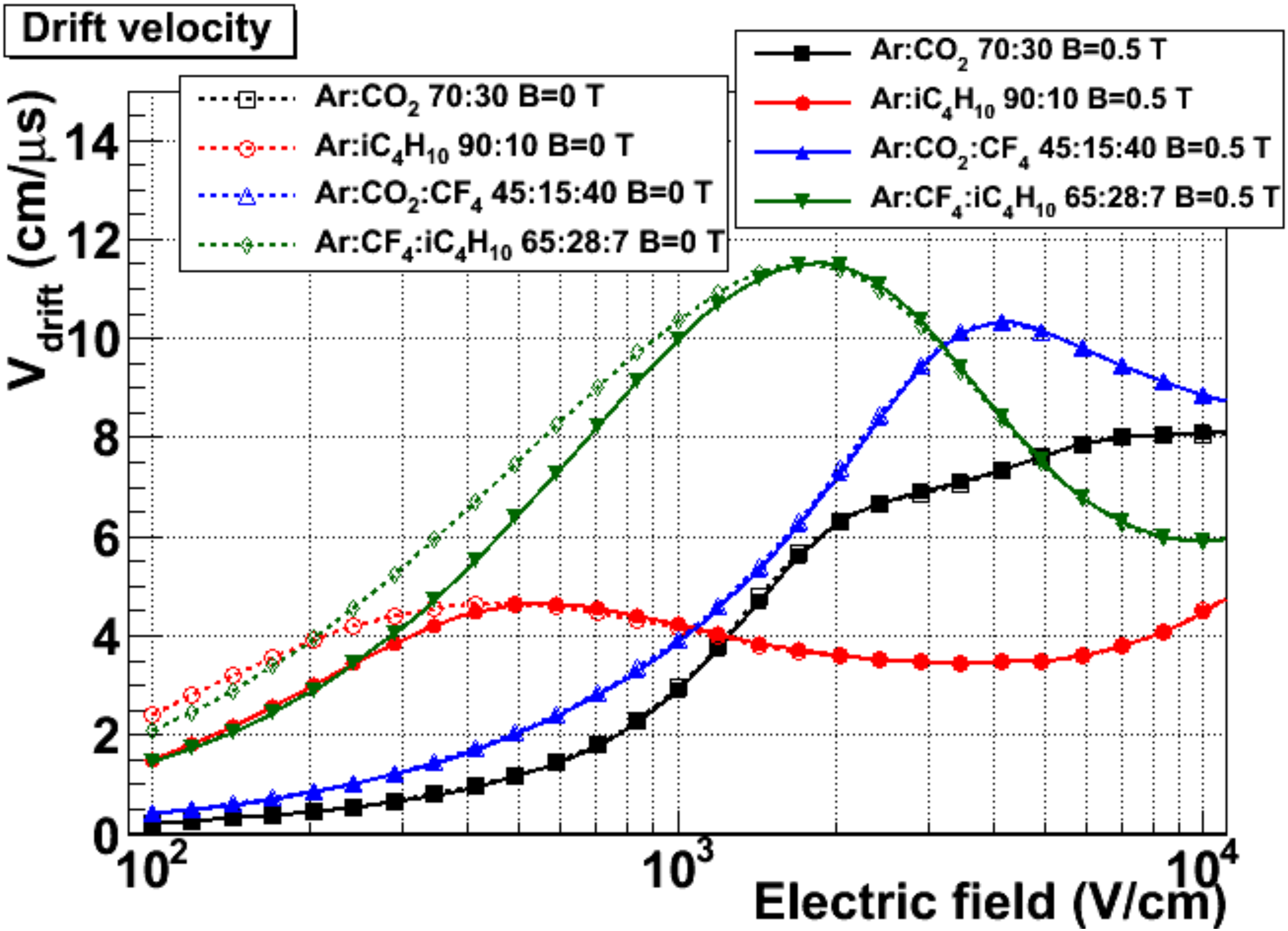

Drift velocity
Ar:CO$_2$ 70:30 B=0 T
Ar:iC$_4$H$_{10}$ 90:10 B=0 T
Ar:CO$_2$:CF$_4$ 45:15:40 B=0 T
Ar:CF$_4$:iC$_4$H$_{10}$ 65:28:7 B=0 T
Ar:CO$_2$ 70:30 B=0.5 T
Ar:iC$_4$H$_{10}$ 90:10 B=0.5 T
Ar:CO$_2$:CF$_4$ 45:15:40 B=0.5 T
Ar:CF$_4$:iC$_4$H$_{10}$ 65:28:7 B=0.5 T
V$_{drift}$ (cm/μs)
0
2
4
6
8
10
12
14
10^2
10^3
10^4
Electric field (V/cm)

The single resistive layer: H4 test beam (2015)

- The devices have been then tested at H4-SPS North Area, equipped with **strips-segmented readout** (400 μm pitch) and **APV25** (CC method, orthogonl tracks)

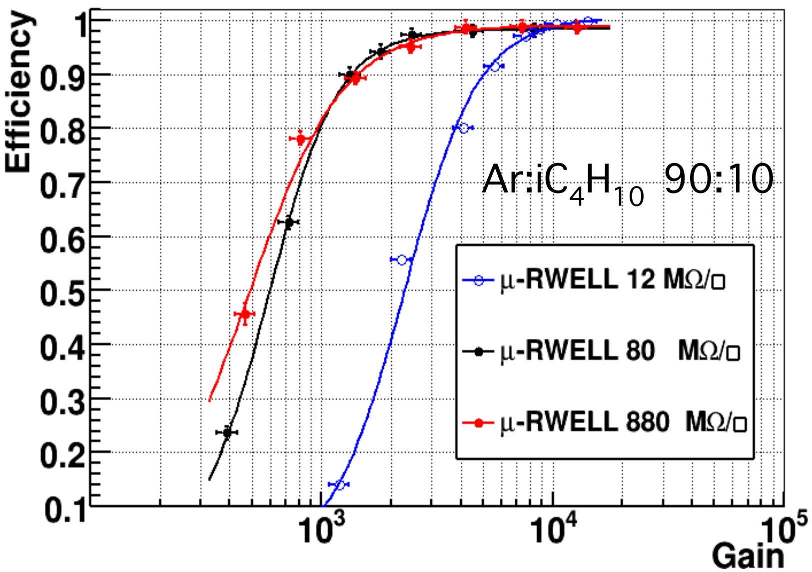

The different behaviour can be assigned to a **different geometry** of the amplification holes, that have not been inspected. At lower resistivity the charge spread more, inducing a weaker signal on the pad. So the gain must be increased to improve the efficiency

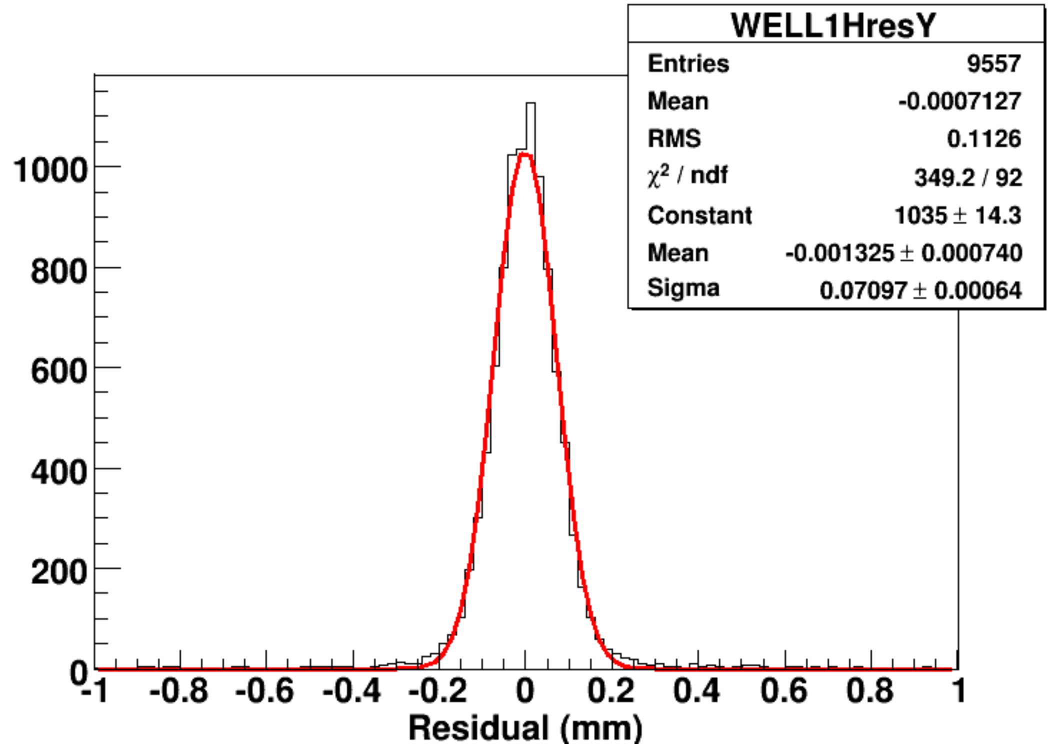

σ_{RWELL} = (52±6) μm

@ B= 0T after TRKs contribution subtraction

The single resistive layer: GIF++ exposure (2017)

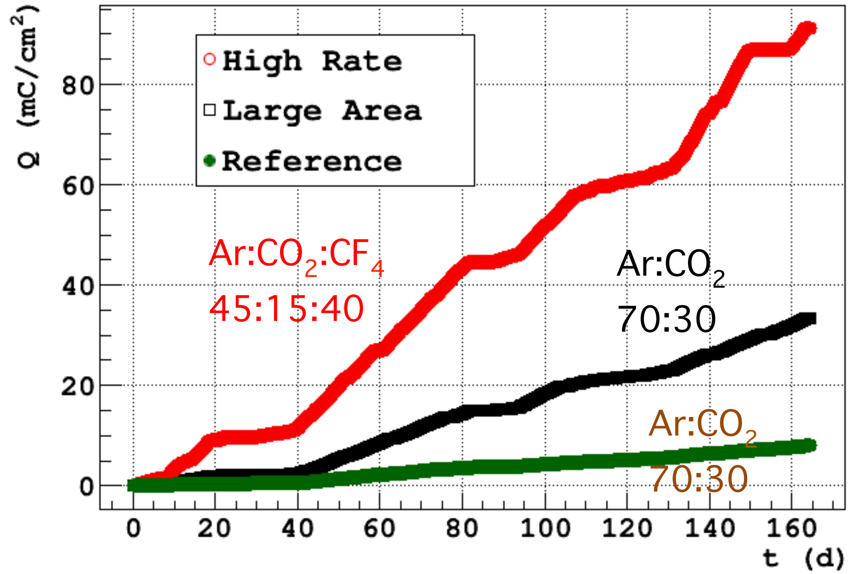

m.i.p. equivalent rate ~10 kHz/cm^2

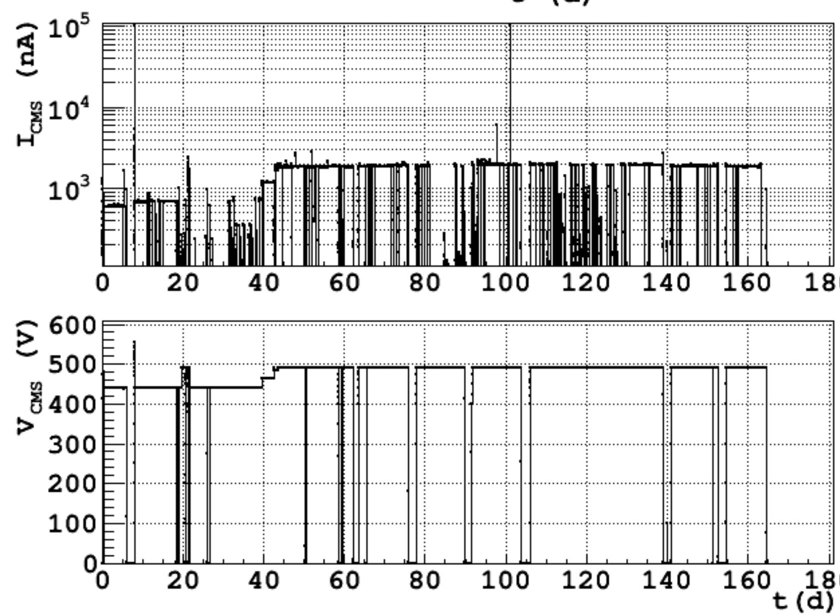

The study of ageing effects on DLC has been done by integrating the charge expected in 10 years of operation in the CMS GE2/1 region (1 kHz/cm^2).

At a gain of 4000 the total charge expected is **2.6 mC/cm^2**

The double resistive layer: H8C test beam (2016)

Two double resistive layer prototypes have been tested with muon beam and equipped with VFAT2

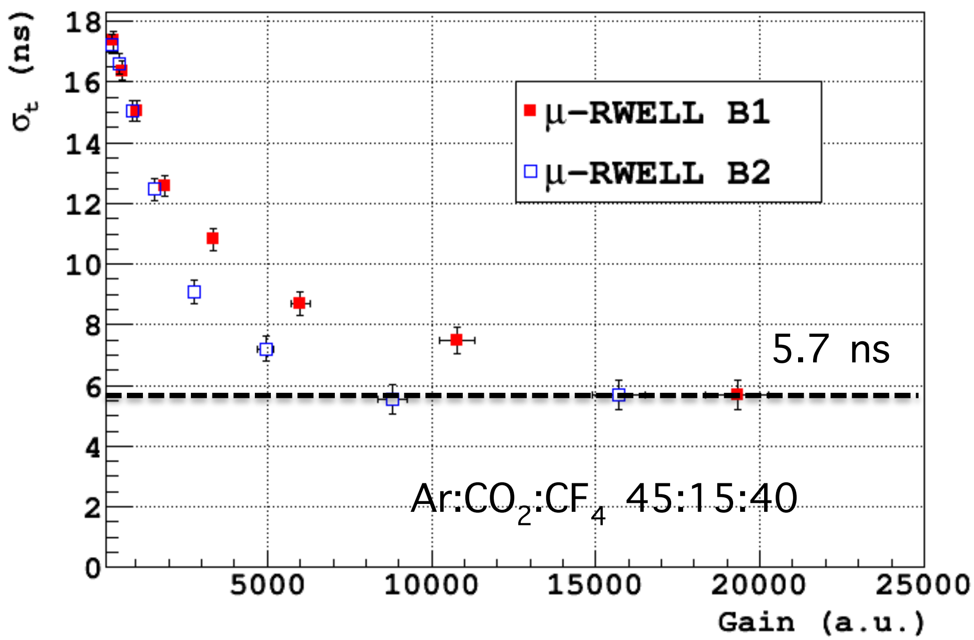

Same saturation observed in GEM detectors operated with the same FEE in the same test beam, while with GEM a time resolution of 4.8 ns has been obtained by LHCb [G. Bencivenni et al., NIM A 494 (2002) 156]

Thanks to L. Benussi, L. Borgonovi, P. Giacomelli, A. Ranieri, M. Ressegotti, I. Vai